Paper

Position-Velocity-Based Trajectory Control for Manipulator and Its Application to Visual Tracking System

Student member Djoko Purwanto (Keio University)

Member Toshiyuki Murakami (Keio University)

Member Kouhei Ohnishi (Keio University)

This paper presents a control system to move the manipulator smoothly in linear path between two designated POSE (position and orientation). Two independent commands, the POSE command and the velocity command, are applied as input of position-based and velocity-based control, respectively. The step function of POSE command describes directly the desired change of manipulator's POSE from a source to a destination POSE. The velocity command determines the desired manipulator velocity, and contributes directly to the smoothness of movement. To obtain a linear path, the trajectories lying between the source and destination POSE are controlled to change in linear way by employing a weighting function. Experiments conducted on a 3-links serial planar manipulator demonstrated the performance of the proposed controller. As addition, taking the merits of the proposed manipulator control system, a visual tracking system is realized and demonstrated via experiments.

Keywords: trajectory planning, trajectory control, motion control, visual tracking

1. Introduction

Obtaining smooth movement with certain constrained trajectories is one of well-known problem in manipulator trajectory planning. Zefran et al. (1998) defines a functional depending on velocity or its derivatives to measure the smoothness of trajectories. By choosing an appropriate measure of smoothness, the trajectories can be determined to satisfy the necessary condition for the shortest distance, minimum acceleration and minimum jerk [5]. Constantinescu et al. (2000) formulates that the desired smoothness of the trajectory is imposed trough limits on the torque rates. Based on translating these limits into state-dependent limits on pseudo-acceleration, an optimization problem by using cubic splines is employed to parameterize the state space trajectory [1].

This paper takes a different perspective comparing to both articles above, proposes a position-velocity-based control method to move the manipulator in linear path between two designated POSE (position and orientation) in workspace scheme. The proposed controller handles directly the common task for manipulator such as "move the manipulator from a source POSE to a destination POSE at certain velocity". The desired change of POSE from a source to a destination is applied directly as command to position-based control. The smoothness of manipulator movement to reach the desired destination POSE is realized by applying a velocity command to velocity-based control. In order to obtain a linear path, the trajectories between the source and the destination POSE should be controlled to change in linear pattern, and it is realized by defining a weighting function employed as part of the control system.

Based on properties described above, the proposed manipulator control system has advantages as follows.

(1) The calculation of intermediate trajectories (between source and destination POSE) is not needed. The intermediate trajectories are generated internally as part of controller.
(2) Command generation is simple. Just apply a new destination POSE and the desired velocity to move the manipulator.
(3) Provide the greater flexibility in combining with other system to build a new system application.

In this paper, several experiments are conducted on 3-links serial planar manipulator to verify the validity of the proposed method. Finally, to show the merits of the proposed control system especially in flexibility to build a new system application, a visual tracking system is also presented.

2. Manipulator Control

In this section, the manipulator control strategy is discussed. The control strategy is designed so that the manipulator can reach the desired POSE (position and orientation) at certain desired velocity via a specific path.

2.1. Workspace Parameters Figure (1) illustrates the workspace parameters definition of the 3-links serial planar manipulator/robot including the end-effector position (x_r, y_r) and orientation α_r. A single camera mounted at the end-effector is used to construct the visual tracking system that will be discussed in next section. In this configuration, the camera's POSE is equal to the manipulator's POSE. The POSE vector in workspace scheme is defined simply as equation (1).

$$\mathbf{h}_R = [\alpha_r \quad x_r \quad y_r]^T \qquad \text{..... (1)}$$

The angular position vector for three joints of manipulator is defined as equation (2) below.

$$\mathbf{q}_R = [\theta_1 \quad \theta_2 \quad \theta_3]^T \qquad \text{..... (2)}$$

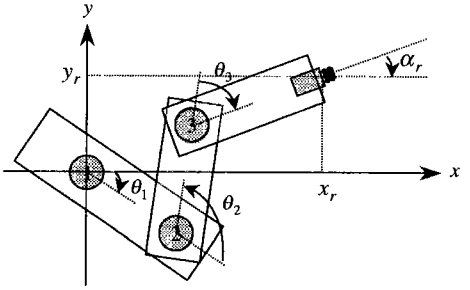

Fig.1. Workspace parameters definition

2.2. Disturbance Observer Disturbance observer is a technique to estimate the disturbance existing in a plant and to make the motion controller to be an acceleration controller. The detail discussion about this topic can be found in article written by Ohnishi et al [2]. Figure (2a) shows the disturbance observer technique applied to a joint motor. The input-output relation of block diagram in figure (2a) is equivalent to a double integrator as shown in figure (2b). Based on the double integrator, the motion controller can be designed easily. Figure (2c) is an example of position control structure applied to double integrator, where the position response depends on the poles location determined by position gain k_p and velocity gain k_v.

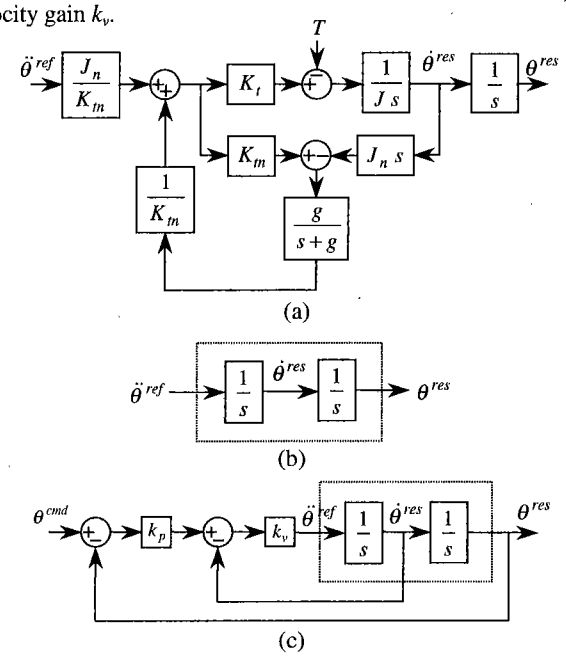

Fig.2. Disturbance observer in a joint motor, its equivalent block, and an example of position control system

2.3. Control Synthesis The proposed position-velocity-based control structure for manipulator is shown in figure (3). This technique is adopted and modified from the control structure in figure (2c). The controller is designed to work in workspace scheme. Two independent inputs are applied in this system and a nonlinear function $NL(\bullet)$ is introduced to handle the control mode. To obtain the joint space acceleration references to be applied as input of disturbance-observer-based acceleration control of the 3-links planar serial manipulator, a joint space acceleration generator is employed. On the contrary, the joint space position and velocity responses are converted to workspace counterpart to obtain the output and the feedback parameters in workspace scheme.

Prior to the detail discussion about the proposed controller, let us define a velocity command vector and a weighting function vector as follows.

$$\mathbf{v}_R^{cmd} = [v_\alpha^{cmd} \quad v_x^{cmd} \quad v_y^{cmd}]^T \qquad \text{..... (3)}$$

$$\mathbf{w}_R = [w_\alpha \quad w_x \quad w_y]^T \qquad \text{..... (4)}$$

$$\mathbf{v}_{RD}^{cmd} = \mathrm{diag}(\mathbf{v}_R^{cmd}) = \begin{bmatrix} v_\alpha^{cmd} & 0 & 0 \\ 0 & v_x^{cmd} & 0 \\ 0 & 0 & v_y^{cmd} \end{bmatrix} \qquad \text{..... (5)}$$

$$\mathbf{w}_{RD} = \mathrm{diag}(\mathbf{w}_R) = \begin{bmatrix} w_\alpha & 0 & 0 \\ 0 & w_x & 0 \\ 0 & 0 & w_y \end{bmatrix} \qquad \text{..... (6)}$$

All of vector components in equations above are positive, and the index α, x, and y express the notation in workspace scheme.

The state space representation of manipulator system in figure (3) is given by equation (7)-(8) below.

$$\dot{\mathbf{z}}_1 = -k_v \mathbf{z}_1 + k_v NL(\mathbf{z}_2, \mathbf{h}_R^{cmd}, \mathbf{v}_R^{cmd}) \qquad \text{..... (7)}$$
$$\dot{\mathbf{z}}_2 = \mathbf{z}_1$$

$$\mathbf{h}_R^{res} = \mathbf{z}_2 \qquad \text{..... (8)}$$

The nonlinear function definition is

$$NL(\mathbf{z}_2, \mathbf{h}_R^{cmd}, \mathbf{v}_R^{cmd}) = \mathbf{w}_{RD}\, \mathbf{v}_{RD}^{cmd}\, \mathrm{sat}\left(k_p (\mathbf{v}_{RD}^{cmd})^{-1} (\mathbf{h}_R^{cmd} - \mathbf{z}_2)\right)$$
$$= \mathbf{w}_{RD}\, \mathbf{v}_{RD}^{cmd}\, \mathrm{sat}\left(k_p (\mathbf{v}_{RD}^{cmd})^{-1} (\mathbf{h}_R^{cmd} - \mathbf{h}_R^{res})\right) \qquad \text{..(9)}$$

k_v and k_p in equations (7) and (9) above are the velocity gain and the position gain, respectively.

The saturation function sat(•) is defined as equation (10).

$$\mathrm{sat}(\varepsilon) = \begin{cases} +1 & \varepsilon > 1 \\ \varepsilon & -1 \le \varepsilon \le 1 \\ -1 & \varepsilon < -1 \end{cases} \qquad \text{..... (10)}$$

Based on the input of nonlinear function, a control mode vector $\mathbf{m}$ that determines weather the manipulator control system is in position-based control mode or in velocity-based control mode, is defined as follows.

$$\mathbf{m} = \mathrm{abs}\left(k_p (\mathbf{v}_{RD}^{cmd})^{-1} (\mathbf{h}_R^{cmd} - \mathbf{h}_R^{res})\right) \qquad \text{..... (11)}$$

The weighting function designed to obtain a linear motion from a source to a destination POSE, is defined in equation (12).

$$\mathbf{w}_R = \begin{cases} \mathbf{1} & \mathbf{m} \le \mathbf{1} \\ \dfrac{\mathrm{abs}\left(\mathbf{h}_R^{cmd} - \mathbf{h}_R^{res}\right)}{\max\left(\mathrm{abs}\left(\mathbf{h}_R^{cmd} - \mathbf{h}_R^{res}\right)\right)} & \mathbf{m} > \mathbf{1} \end{cases} \qquad \text{..... (12)}$$

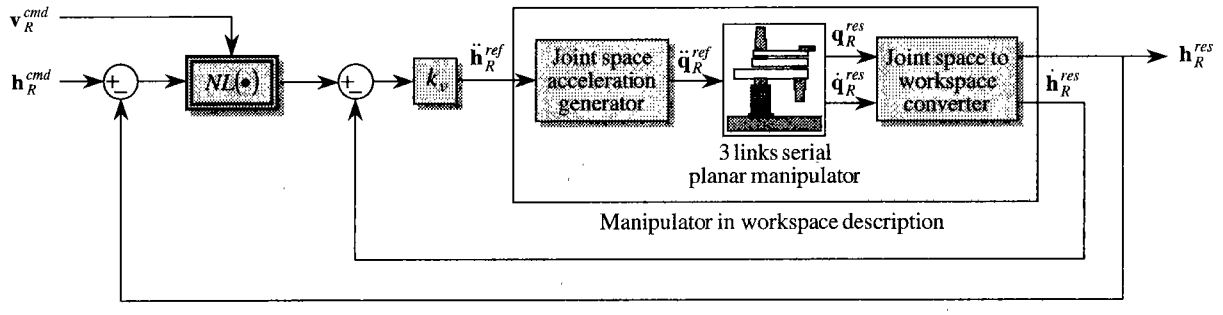

Fig.3. Position-velocity-based control for manipulator

In real application, the value of max(abs(•)) in equation (12) above is an instantaneous maximum value calculated at every sampling time.

The position-based control mode happens when the POSE response $\mathbf{h}_R^{res}$ is close to the POSE command $\mathbf{h}_R^{cmd}$, and it is expressed in equation (13).

$$\mathbf{m} \le \mathbf{1} \quad \text{or} \quad \text{abs}\left(\mathbf{h}_R^{cmd} - \mathbf{h}_R^{res}\right) \le \text{abs}(\mathbf{v}_R^{cmd} / k_p) \quad \ldots\ldots\ldots\ldots (13)$$

If condition in equation (13) is satisfied, by using the weighting function as defined in equation (12), the nonlinear equation (9) can be simplified as follows.

$$\begin{aligned} NL(\mathbf{z}_2, \mathbf{h}_R^{cmd}, \mathbf{v}_R^{cmd}) &= k_p\,(\mathbf{h}_R^{cmd} - \mathbf{z}_2) \\ &= k_p\,(\mathbf{h}_R^{cmd} - \mathbf{h}_R^{res}) \end{aligned} \quad (\mathbf{m} \le 1) \quad \ldots\ldots\ldots (14)$$

Substitute equation (14) to equation (7), a simple linear state space equation as expressed in equation (15)-(16) is obtained. These equations describe the manipulator control system with ordinary position-based control configuration. Figure (4) illustrates the block diagram of manipulator control system in position-based control mode. Here, the POSE response $\mathbf{h}_R^{res}$ depends only on the POSE command $\mathbf{h}_R^{cmd}$.

$$\dot{\mathbf{z}}_1 = -k_v\,\mathbf{z}_1 - k_v\,k_p\,\mathbf{z}_2 + k_v\,k_p\,\mathbf{h}_R^{cmd} \quad \ldots\ldots\ldots\ldots (15)$$

$$\dot{\mathbf{z}}_2 = \mathbf{z}_1$$

$$\mathbf{h}_R^{res} = \mathbf{z}_2 \quad \ldots\ldots\ldots\ldots (16)$$

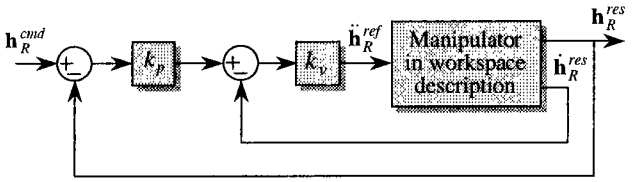

Fig.4. Position-based mode control system

On the other hand, if the control mode vector becomes large ($\mathbf{m} > \mathbf{1}$) or the POSE response is far from the POSE command, the manipulator control system changes to the velocity-based control mode. In this condition, the nonlinear equation (9) can be simplified as equation (17). Here, due to the value of control mode vector $\mathbf{m}$ is relative large, the saturation function can be replaced by the signum function.

$$\begin{aligned} NL(\mathbf{z}_2, \mathbf{h}_R^{cmd}, \mathbf{v}_R^{cmd}) &= \mathbf{w}_{RD}\,\mathbf{v}_{RD}^{cmd}\,\text{sign}(\mathbf{h}_R^{cmd} - \mathbf{z}_2) \\ &= \mathbf{w}_{RD}\,\mathbf{v}_{RD}^{cmd}\,\text{sign}(\mathbf{h}_R^{cmd} - \mathbf{h}_R^{res}) \end{aligned} \quad (\mathbf{m} > 1) \ldots (17)$$

In velocity-based control mode, the POSE response depends on three parameters, the POSE command $\mathbf{h}_R^{cmd}$, the velocity command $\mathbf{v}_R^{cmd}$, and the weighting function $\mathbf{w}_R$. The POSE command guides the movement direction, and the velocity command determines the smoothness of movement. The weighting function synchronizes the velocity so that the all component of POSE response vector changes to reach the POSE command in same settling time and in linear way. The mechanism described above eliminates the calculation procedure to determine the intermediate trajectories.

To build a real application, the position gain k_p and velocity gain k_v should be chosen properly. Both of parameters of k_p and k_v determine the pole location in position-based control mode and consequently determine the transient response in this control mode. Meanwhile, the pole location and the transient response of velocity-based control is only determined by velocity gain k_v. Setting of $k_v = 4\,k_p$ is a normal choice to produce two poles in same location for position-based control system. Furthermore, as described in equation (13), the position gain k_p also determines the transition point between position-based and velocity-based control mode. Generally, the transient response in both position and velocity control mode should be slower than the transient response in disturbance observer-based acceleration control applied to each joint of manipulator.

3. Visual Tracking System

The flexibility in constructing a new system application using the proposed control for manipulator is shown here by building a visual tracking system. In this tracking system, the manipulator tracks the object in certain desired configuration.

3.1. Basic Operation Modes The visual tracking system has two operation modes as follows.

(1). The single destination tracking mode as described in figure (5a), where the manipulator move to a destination POSE (position and orientation) at certain velocity $\mathbf{v}$ to satisfy the desired configuration with respect to the object's POSE.

(2) The continuous tracking mode as shown in figure (5b), where the manipulator moves to satisfy the desired configuration with respect to the moving object.

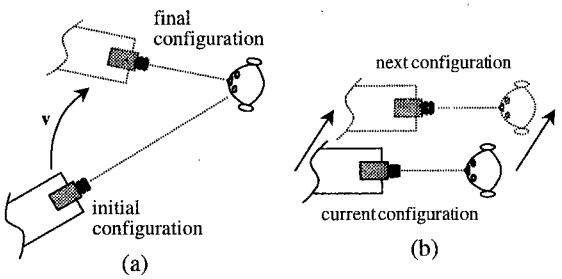

Fig.5. Visual tracking illustration

3.2. Object Measurement The aim of object measurement is to determine the manipulator-object relation parameters. As illustrated in figure (6), the parameters include the measurement of object's angle (ϕ^m), distance (d^m), and deviation (δ^m) with respect to the manipulator.

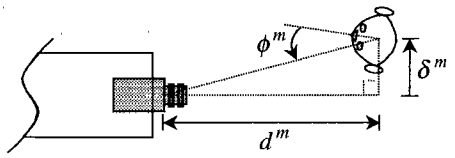

Fig.6. Manipulator-object relation parameters

Figure (7) shows the signal flow to determine the manipulator-object relation parameters. The change of object's pattern in image plane is used to obtain the angle information. The normalization procedure is employed to simplify the pattern analysis. The normalized pattern is then analyzed by the neural-network technique to obtain the object's angle. The convenient structure to manage the balance between the accuracy degree of analysis and the required time processing via the normalized pattern size and the number of hidden nodes, is the main reason to utilize the neural-network-based angle measurement. Meanwhile, to obtain the distance and the deviation information, the geometrical calculation based on camera's focal length as illustrated in figure (8) is used.

The multi-layer neural network structure including an input layer,

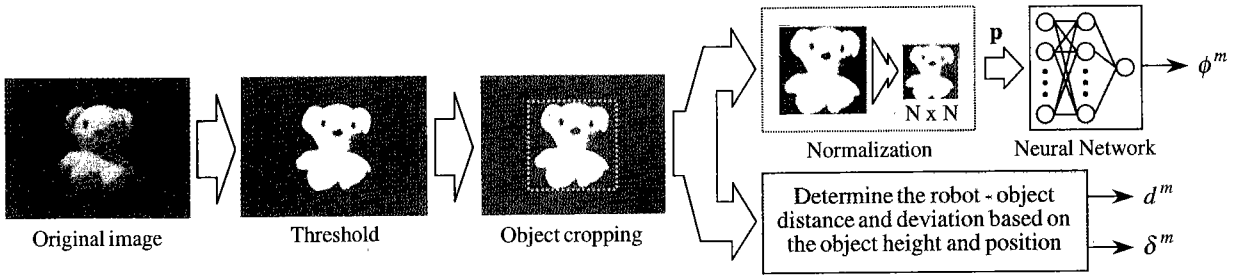

Fig.7. Signal flow for object measurement

one hidden layer and an output layer, is used to determine the object's angle. The input-output relation of the network is given by equation (18). The weights and bias are adjusted offline using backpropagation method.

$$\phi^m = \mathbf{w}_H \, \sigma(\mathbf{w}_I \, \mathbf{p} + \mathbf{b}_I) \quad \cdots\cdots (18)$$

Here, $\mathbf{w}_H$, $\mathbf{w}_I$, and $\mathbf{b}_I$ are the weight in hidden layer, weight in input layer, and bias in input layer, respectively. The function $\sigma(\bullet)$ is a unipolar sigmoid function defined as equation (19). The input vector $\mathbf{p}$ is the normalized image data information with dimension NxN.

$$\sigma(\beta) = \frac{1}{1+e^{-\beta}} \quad \cdots\cdots (19)$$

The distance and deviation measurement given by equation (20)-(21), are calculated based on the triangle properties as shown in figure (8).

$$d^m = f + \frac{f\,Y_O}{\lambda_y \, p_y} \quad \cdots\cdots (20)$$

$$\delta^m = -f \frac{\lambda_x \, p_x}{\lambda_y \, p_y} Y_O \quad \cdots\cdots (21)$$

Here, f is focal length, Y_O is the pre-known object height. λ_x, λ_y and p_x, p_y are the scaling factor and the pixel size in x and y direction, respectively. The minus sign in equation (21) is required to satisfy the manipulator-object relation definition as describe in figure (6).

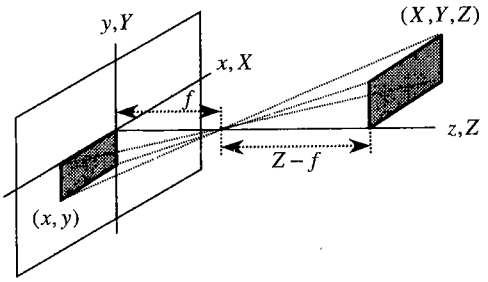

Fig.8. Triangle principle to determine the object's distance and deviation

To simplify the notation, we define a general manipulator- object relation vector as equation (22) below.

$$\mathbf{r} = [\phi \quad d \quad \delta]^T \quad \cdots\cdots (22)$$

If $\mathbf{h}_R^a$ denotes the actual POSE of manipulator, and $\mathbf{i}$ denotes the visual information, due to the placement of camera at the end-effector of manipulator, the measurement of manipulator-object relation parameters can be expressed simply as follows.

$$\mathbf{r}^m = f_1(\mathbf{h}_R{}^a, \mathbf{i}) \quad \cdots\cdots (23)$$

3.3. Object Estimation Object estimation is a process to obtain the estimation value of object's POSE. The estimation values are determined based on the geometrical relation of the manipulator's POSE and the measurement of manipulator-object relation parameters (angle, distance, and deviation).

Figure (9) illustrates the geometric description to estimate the object's POSE. Here, the estimation of object's POSE can be written as equation (24)-(25).

Object orientation:

$$\hat{\alpha}_o = \alpha_r{}^a + \phi^m - \tan^{-1}(\delta^m / d^m) \quad \cdots\cdots (24)$$

Object position:

$$\begin{bmatrix} \hat{x}_o \\ \hat{y}_o \end{bmatrix} = \begin{bmatrix} x_r{}^a \\ y_r{}^a \end{bmatrix} + \begin{bmatrix} \cos\alpha_r{}^a & \sin\alpha_r{}^a \\ -\sin\alpha_r{}^a & \cos\alpha_r{}^a \end{bmatrix} \begin{bmatrix} d^m \\ \delta^m \end{bmatrix} \quad \cdots\cdots (25)$$

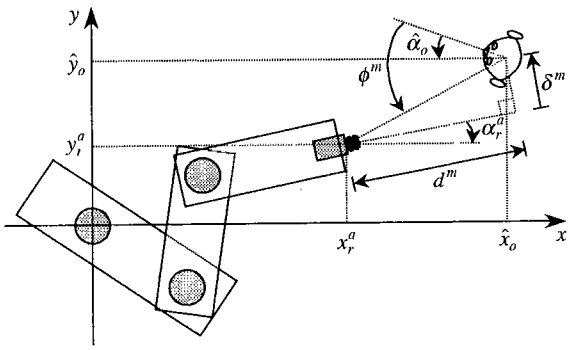

Fig.9. Object's POSE estimation

The object's POSE vector $\mathbf{h}_O$ is given by following equation.

$$\mathbf{h}_O = [\alpha_o \quad x_o \quad y_o]^T \quad \cdots\cdots (26)$$

In simple notation, the estimation of object's POSE in equation (24)-(25) can be expressed simply as follows.

$$\hat{\mathbf{h}}_O = f_2(\mathbf{h}_R{}^a, \mathbf{r}^m) \quad \cdots\cdots (27)$$

3.4. Destination POSE of Manipulator Destination POSE is the desired POSE for manipulator. It is calculated based on the

estimated object's POSE as given by equation (27) and the desired manipulator-object relation parameters (desired angle, distance, and deviation). Figure (10) and equation (28)-(29) show the method to calculate the destination POSE of manipulator.

Manipulator orientation:

$$\alpha_r^{dst} = \hat{\alpha}_o - \phi^d + \tan^{-1}\left(\delta^d / d^d\right) \quad \text{..... (28)}$$

Manipulator position:

$$\begin{bmatrix} x_r^{dst} \\ y_r^{dst} \end{bmatrix} = \begin{bmatrix} \hat{x}_o \\ \hat{y}_o \end{bmatrix} + \begin{bmatrix} -\cos\alpha_r^{dst} & -\sin\alpha_r^{dst} \\ \sin\alpha_r^{dst} & -\cos\alpha_r^{dst} \end{bmatrix} \begin{bmatrix} d^d \\ \delta^d \end{bmatrix} \quad \text{..... (29)}$$

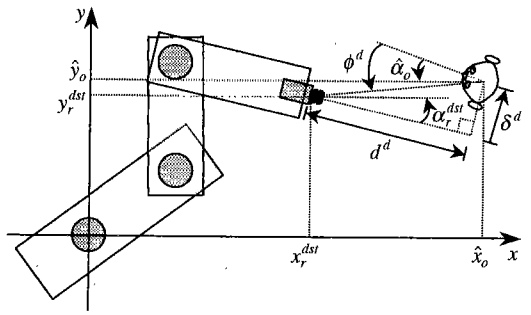

Fig.10. Destination POSE calculation

The destination POSE of manipulator in equation (28)-(29) above can be expressed as follows.

$$\mathbf{h}_R^{dst} = f_3\left(\hat{\mathbf{h}}_O, \mathbf{r}^d\right) \quad \text{..... (30)}$$

3.5. Visual Tracking Structure Figure (11) shows the proposed visual tracking system block diagram. In this tracking system, the calculation result of destination POSE is applied directly as POSE command. On the other hand, the POSE response is taken as the actual POSE of manipulator system. By setting the velocity command to a constant value, the input-output relation of "manipulator and control" block can be expressed as follows.

$$\mathbf{h}_R^a = f_4\left(\mathbf{h}_R^{dst}\right) \quad \text{..... (31)}$$

The visual tracking system can be constructed by combining equation (23), (27), (30) and (31). The input $\mathbf{r}^d$ including the desired angle-distance-deviation of the object with respect to the manipulator/camera represents the desired configuration in the tracking system. The image information **i** (captured by camera mounted at the end-effector) generates the current configuration. The velocity command $\mathbf{v}_R^{cmd}$ determines the saturation speed of manipulator. Generally, the velocity command can be set to any value either in fixed value of as time function, as long as the manipulator movement cause no visual effect in image capturing such as blurring, and so on. Based on the difference between desired and current configuration, and the saturation speed, the tracking system is controlled to satisfy the desired configuration.

In practical implementation, the control technique as illustrated on figure (3) is executed at relative short sampling time (typically 1 ms). On the other hand, in the tracking system as figure (11), the visual perception needs the longer time processing to obtain the object parameters, and it leads the input command for manipulator control system to change at every image sampling time in step transition form.

4. Experiments

4.1. Experimental System Figure (12) shows the experimental environment including the 3-links serial planar manipulator, a bear doll used as object in visual tracking system, and a joystick to move the object freely. Figure (13) shows the software and hardware description and signal flow diagram for experimental purpose. Table (1) shows the parameters setting for manipulator and control.

4.2. Experimental Results of Manipulator Control Figure (14) shows the experimental results of the proposed control system for manipulator with various POSE (position and orientation) command and velocity command. At t<18 sec, the velocity command for both x and y direction is set to 0.1 m/sec. At t=10 sec, a step POSE command in x and y direction changes at 0.2 meters in distance, and the POSE response reaches the POSE command setting at around 2.2 seconds in linear way. It means that the manipulator moves at velocity around 0.2/2.2=0.0909 m/sec for both x and y direction, close enough to 0.1 m/sec of the velocity command setting.

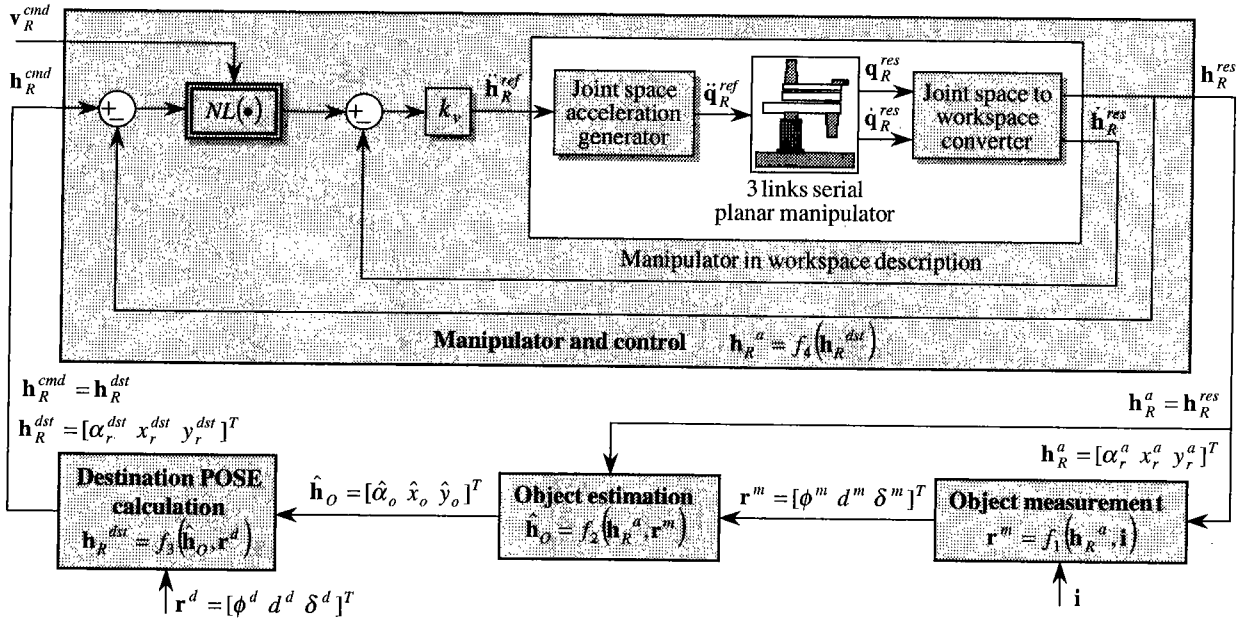

Fig.11. Visual tracking system realization

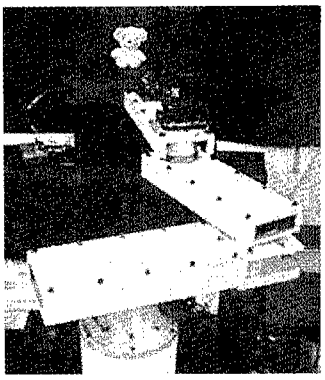

Fig.12. Experimental environment

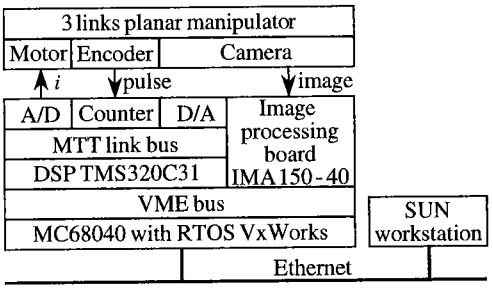

Fig.13. Signal flow diagram

Table (1) Parameters setting for manipulator control

Parameter	Notation	Value
position gain	k_p	10
velocity gain	k_v	40
length of link	(L_1, L_2, L_3)	(0.25, 0.26, 0.33) [m]
sampling time	t_s	1 [msec]

At t=20 sec, with 0.05 m/sec of the velocity command, the POSE command changes only in y direction at 0.2 meters in distance. As result, the POSE response reaches 0.2 meters at around 3.8 seconds. In other word, it can be said that the manipulator velocity is 0.2/3.8=0.0526 m/sec, and satisfies the velocity command setting that is 0.05 m/sec.

Finally, at t=30 sec, the POSE command changes only in α direction, and again the transition velocity of the POSE response satisfies the velocity command in α direction.

The effect of linear transition in manipulator movement is shown by figure (15) and (16). Figure (15) illustrates the manipulator posture from t=10 sec to t=13 sec when the manipulator's POSE changes in x and y direction [see also the figure (14)]. Furthermore, figure (16) illustrates the manipulator posture from t=30 sec to t=33 sec when the manipulator's POSE changes only in α direction. The thin line and the thick line indicate the initial POSE and the final POSE, respectively.

In general, the experimental results show that the velocity command has important role to determine the POSE response transition to reach the desired value. Another important result is the linear transition that shows the significant role of the weighting function.

4.3. Experimental Results of Object Measurement In this experiment, we employ the 32x32 normalized data for input layer of the neural-network-based angle measurer, and operate 6 nodes in hidden layer to perform object's angle measurement. Table (2) describes the experimental results in measuring the manipulator-object relation parameters. The standard deviation value indicates that the accuracy of deviation measurement is relative good comparing to the angle and the distance measurement. A number of similar experiments with different condition produces similar trend. The experimental results show that a small amount of noise exists in

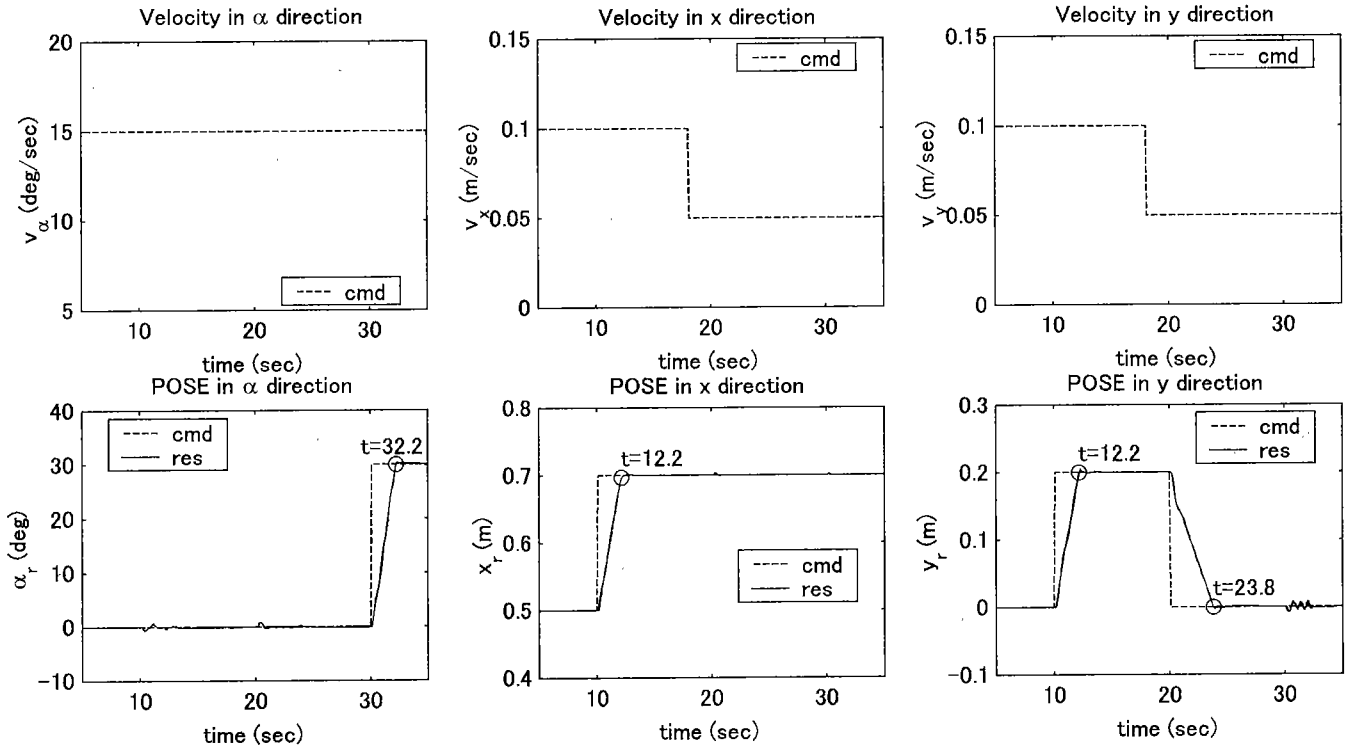

Fig.14. Experimental result of manipulator control

measurement system.

The other important factor in visual measurement process is the processing time, especially for angle measurement. Table (3) shows the calculation time of angle measurement. The calculation time is proportional to the number of input nodes and hidden nodes.

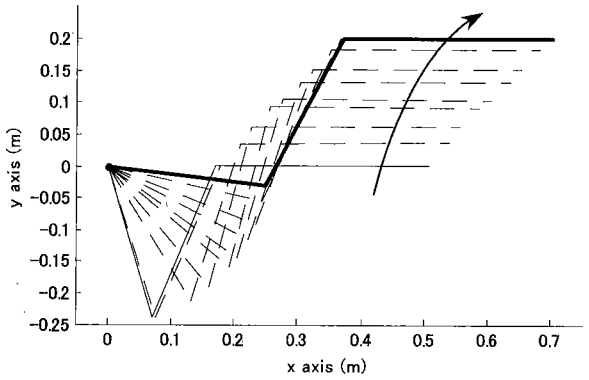

Fig.15. Manipulator posture (t=10~13 sec)

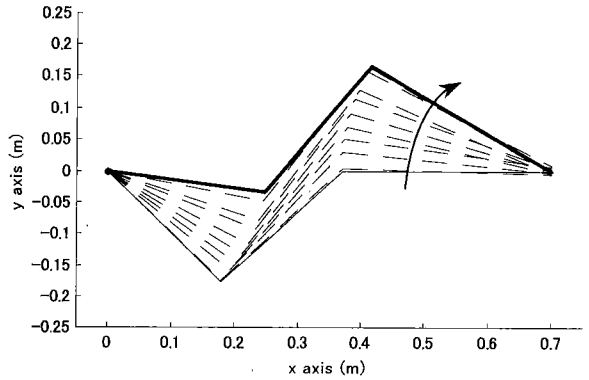

Fig.16. Manipulator posture (t=30~33 sec)

Table (2) Object measurement in certain condition

Measurement	Desired value	Mean	Standar deviation
angle	0 deg	–0.27 deg	0.9658 deg
distance	0.5 m	0.5 m	0.0026 m
deviation	0 m	0 m	0 m

Table (3) Calculation time of angle measurement

Input nodes (NxN)	Hidden nodes	Calculation time
32 x 32	6	105.6 msec
32 x 32	12	111.6 msec
32 x 32	24	123.9 msec

4.4. Experimental Results in Visual Tracking System In this experiment, the parameters setting for manipulator and control as shown in table (1) is used. For neural-network-based angle measurement in visual perception process, we employ the 32x32 of normalized data for input layer and the six nodes of hidden layer. The visual measurement process is synchronized to 150 msec fixed sampling rate. All of velocity command for manipulator is set to constant values that are 0.05 rad/sec in α direction, 0.05 m/sec in x direction, and 0.05 m/sec in y direction.

Figure (17) shows the experimental result of visual tracking system. Here, the desired manipulator-object configuration expressed by vector $\mathbf{r}^d$ changes at a certain time, and results the measurement vector $\mathbf{r}^m$. At t=14 sec, both of the desired angle and the desired distance change to a new desired values. The measurement results show that the desired setting is reached at about 3 seconds. The similar trend is also shown when the desired angle changes at t=29 sec. Based on the fact that the dynamic relation in the tracking system lies only in "manipulator and control" block, the measurement results expressed in figure (17) confirm that the transition to reach the desired values depend on the velocity commands setting for manipulator. Furthermore, due to the imperfect measurement process that produce a certain amount of noise, the vibration effect exists in the tracking system.

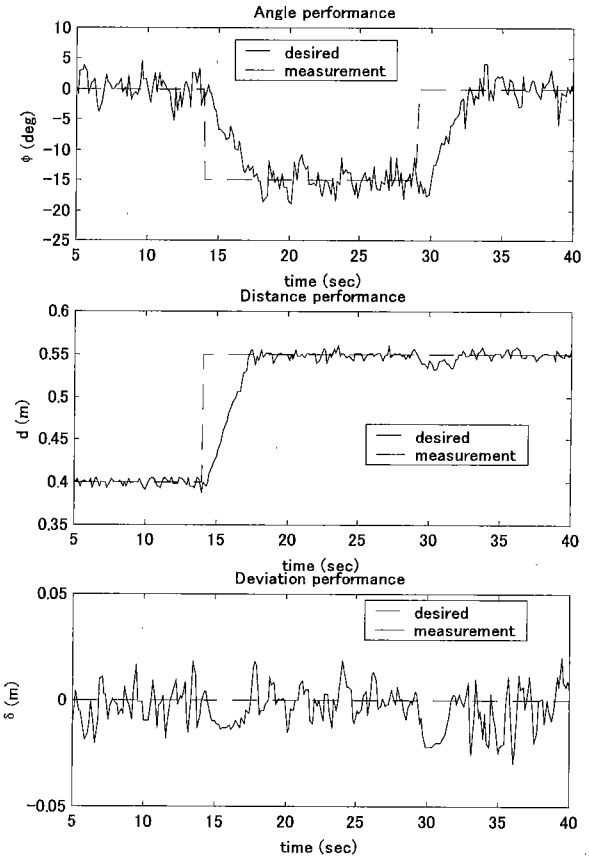

Fig.17. Performance of visual tracking system

Figure (18) illustrates the situation of manipulator and object configuration when the desired angel and the desired distance change to new setting (t=14 sec to t=18 sec). Furthermore, figure (19) describes the condition when only the desired angel changes to new setting (t=29 sec to t =33 sec).

In general, the experimental results confirm that the tracking system can work properly under certain amount of vibration condition due to the noise appearing in visual measurement process.

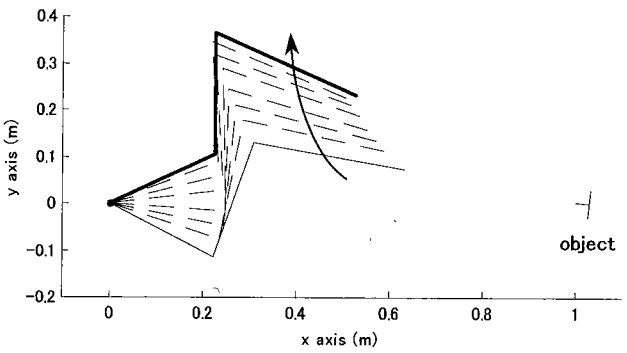

Fig.18. Tracking condition at t=14~18 sec

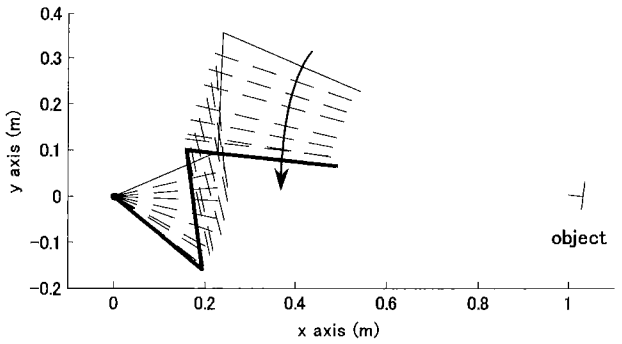

Fig.19. Tracking condition at t=29~33 sec

5. Conclusion

The position-velocity-based trajectory control for manipulator and its application to visual tracking system was presented. Employing the velocity command and the weighting function beside the POSE (position and orientation) command, eliminate the requirement to calculate the intermediate trajectories. Simple command generation, no need calculation of intermediate trajectories, and high flexibility to construct a new system application, are the main advantages of this proposed method. Several experimental results verified the proposed approach.

(Manuscript received Oct. 2, 2000, revised March 6, 2001)

References

(1) Constantinescu D. and Croft EA, Smooth and time- optimal trajectory planning for industrial manipulators along specified paths, *Journal of Robotic Systems*, Vol. 17, No. 5, pp. 233-249 (2000)
(2) K. Ohnishi, M. Shibata, and T. Murakami, Motion control for advance mechatronics, *IEEE/ASME Transaction on Mechatronics*, Vol.1 No.1, pp. 56-67 (1996)
(3) Kieffer J, Cahill AJ, and James MR, Robust and accurate time-optimal path-tracking control for robot manipulators, *IEEE Transaction on Robotic and Automation*, Vol. 13, No. 6, pp. 880-890 (1997)
(4) Seth Hutchinson, Gregory D. Hager, and Peter I. Corke, A tutorial on visual servo control, *IEEE Transaction on Robotic and Automation*, Vol. 12, No. 5, pp. 651-670 (1996)
(5) Zefran M, Kumar V, and Croke CB, On the generation of smooth three-dimensional rigid body motion, *IEEE Transaction on Robotic and Automation*, Vol. 14, No. 4, pp. 576-589 (1998)

Djoko Purwanto (Member) received B.E. degree in electrical engineering from Institute of Technology "Sepuluh Nopember" Surabaya, Indonesia, in 1989. The M.E. degree in electrical engineering was received from Keio University in 1999. He is currently working towards Ph.D. degree at Keio University. His research interests include image processing, motion control, and robotic vision.

Toshiyuki Murakami (Member) received B.E., M.E., and Ph.D. degrees in electrical engineering form Keio University in 1988, 1990, and 1993, respectively. Since 1993, he has been with Keio University. His research interests include robotics, micromechatronics, and motion control.

Kouhei Ohnishi (Member) received B.E., M.E., and Ph.D. degrees, all in electrical engineering from the University of Tokyo in 1975, 1977, and 1980, respectively. Since 1980, he has been with Keio University. His research interests include mechatronics, motion control and robotics. Dr. Ohnishi is an IEEE Fellow for contributions to the development of disturbance observer and its applications to motion control.